https://doi.org/10.5194/egusphere-2026-801
Preprint. Discussion started: 13 March 2026

Measurement report: Investigation of regional pollutant transport to Beijing, China based on a unique 528-meter platform

Xiaoxue Liu[1,2 §], Pengkun Ma[2 §], Yubing Pan[2], Qianqian Wang[2], Pengfei Tian[1,*], Lei Zhang[1], Jiannong Quan[2,*]

[1]Colledge of Atmospheric Sciences, Lanzhou University, Lanzhou, China
[2]Institute of Urban Meteorology, Chinese Meteorological Administration, Beijing, China.
[§]These two authors contributed equally.

Correspondence to:
Jiannong Quan, jnquan@ium.cn
Pengfei Tian, tianpf@lzu.edu.cn

https://doi.org/10.5194/egusphere-2026-801
Preprint. Discussion started: 13 March 2026

Abstract

Observations at elevated altitudes can capture the chemical characteristics of regional aerosols more effectively than ground-level measurements, but in situ measurements of aerosols over megacities remain scarce. In this work, aerosol composition and gaseous pollutants measured from 2020 to 2024 at a 528-m landmark tower in downtown Beijing, together with ground-level observations, are analyzed to understand regional pollutant transport. The results reveal that both aerosol mass concentration and composition differ significantly among air masses originating from different directions. Further analysis of sulfur and nitrogen oxidation ratios showed that both were significantly higher in air masses from the south and northeast compared to those from the northwest. This difference is likely attributable to higher relative humidity (RH) in the former, which promotes heterogeneous oxidation of SO_2 and NO_2 during transport. Regional aerosols were downwards transported to ground efficiently through planetary boundary layer (PBL) process during daytime, thereby exacerbating air pollution in Beijing. These findings underscore the critical role of regional transport in shaping Beijing's aerosol burden and highlight how the chemical signatures of transported aerosols reflect their diverse source regions and formation mechanisms.

Short summary

Regional transport is a systemic environmental challenge governed by multiple processes. Observations from a unique 528-m tower in Beijing reveal that aerosols vary among air masses originating from different directions, influenced by regional emission sources and reactions during transport. A comparison of pollutants between the 528-m layer and ground level confirms that transported pollutants are mixed down to the surface during daytime, governed primarily by planetary boundary layer process.

1. Introduction

The megacity of Beijing and the surrounding North China Plain (NCP) constitute one of the world's most polluted and intensively studied regions for regional air pollution dynamics, owing to its dense population, rapid industrialization, and complex meteorology (Li et al., 2016). In addition to local emissions, regional transport is a major contributor to Beijing's air pollution. Model simulations indicate that the regional contribution to $PM_{2.5}$ in Beijing ranges from 27% to 78% and has been increasing annually (Li et al., 2013; Zhang et al., 2018, 2024). This contribution is particularly important during haze events, when regional transport has sometimes been identified as the primary driver. Observation-based studies further show that pollutants such as SO_2 and $PM_{2.5}$ are transported northwards along the Taihang mountains, exacerbating air pollution in Beijing (Li et al., 2015; Tan et al., 2021). These studies underscore that mitigating Beijing's air pollution cannot rely on local emission controls alone (Li et al., 2015).

Regional pollutant transport is not merely a local environmental issue but a systemic

https://doi.org/10.5194/egusphere-2026-801
Preprint. Discussion started: 13 March 2026

atmospheric process governed by interactions among anthropogenic emissions, synoptic-scale weather patterns, topographic constraints, and PBL process (Li et al., 2016). Among these processes, the vertical transport between the PBL and free troposphere (FT) is critically important, but remains poorly understudied. This gap stems largely from the need for vertical profiling of atmospheric pollutants to fully characterize the composition and evolution of aerosols—a requirement that poses significant challenges for observational systems, as most measurements have been conducted at ground level. Regional pollutant transport occurs more efficiently in the lower FT, which is supported by both observations and model simulations. Quan et al. (2020) observed an elevated pollutant layer (EPL) at an altitude of 1.4-1.7 km over Beijing by lidar and aircraft measurements. Model simulations indicate the EPL in the lower FT formed over the NCP due to a mountain-induced vertical vortex and was subsequently transported to Beijing by southerly winds. Sun et al. (2022) observed high concentrations of sulfate-dominated aerosols in the FT over Northeast China, in contrast to the low aerosol loadings—primarily composed of organic compounds—in the PBL. Model simulations indicate that these elevated pollutants in the lower FT were transported directly from the North China Plain (NCP) by warm, moist air masses. While downward transport of pollutants from the FT to the PBL may be influenced by PBL process or local circulation, the underlying mechanisms remain poorly understood.

Moreover, the chemical composition of aerosol varies substantially in different regions, depending on emission sources and atmospheric chemical reactions. For example, coal combustion emits SO_2, which is oxidized in the atmosphere to form sulfate, while vehicle exhaust releases NO_x, a precursor to nitrate. Numerous studies utilizing the Hybrid Single-Particle Lagrangian Integrated Trajectory (HYSPLIT) model have demonstrated that synoptic-scale meteorology strongly influences the chemical characteristics of particulate matter in Beijing (Ma et al., 2021; Kang et al., 2023). For instance, air masses arriving from southern and southeastern industrial corridors, including provinces such as Hebei, Shandong, and Henan, are consistently associated with elevated concentrations of SIAs, including nitrate (NO_3^-), sulfate (SO_4^{2-}), and ammonium (NH_4^+), due to high precursor emissions of NO_x, SO_2, and NH_3 from coal combustion, vehicle exhaust, and agricultural activities (Du et al., 2019). Conversely, air masses originating from northern or northwestern regions, such as Inner Mongolia or the Gobi Desert, are typically linked to dust-laden conditions and higher contribution of mineral dust components to aerosol loading (Wang et al., 2017). Notably, most observations are conducted at ground level, where local and transported pollutants are well mixed. Aircraft observations showed that aerosol compositions varied drastically with altitude, especially near the top of PBL (Liu et al., 2019). Therefore, observations in high layer may capture chemical characteristics of transported aerosols from different regions much better.

To address these research gaps, aerosol composition and gaseous pollutants measured from 2020 to 2024 at a 528-m landmark tower in downtown Beijing, together with

https://doi.org/10.5194/egusphere-2026-801
Preprint. Discussion started: 13 March 2026

ground-level observations of pollutants such as NO_2, SO_2, and $PM_{2.5}$, are analyzed in this study to understand regional pollutant transport to Beijing and thereby improve our understanding of near-surface air pollution.

2. Observations and Methods

The comprehensive field campaign was conducted from October 2020 to December 2024 on the roof of the 528-m CITIC Tower. The CITIC Tower is situated adjacent to the East Third Ring Road (Fig.1), in a mixed residential and commercial area with no large point source nearby. The measurements included aerosol mass concentration and composition (SO_4^{2-}, NO_3^-, NH_4^+, Chl^-, and organic aerosols (Org)), trace gases (SO_2, NO_2, CO, O_3), and meteorological variables.

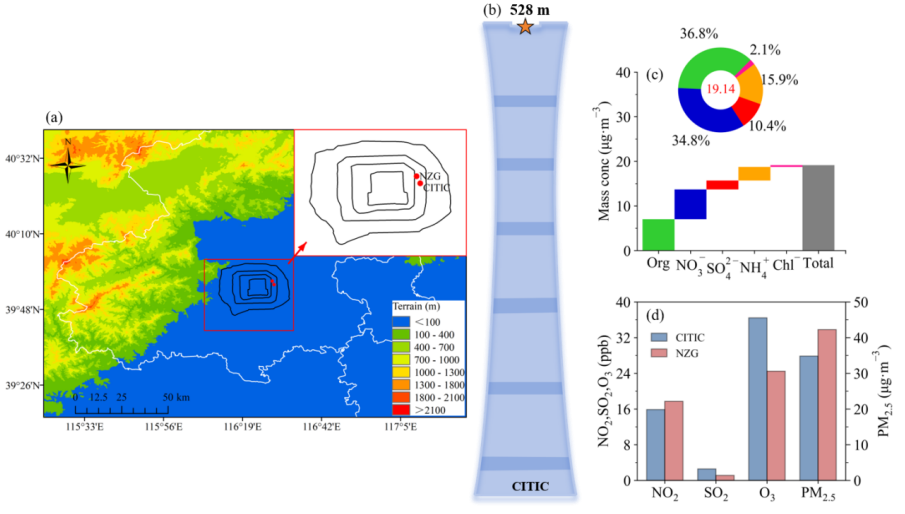

Figure 1. Locations of the monitoring sites used in this study with lack lines, red dots representing the second to fifth rings surrounding central Beijing, and CITIC and NZG stations, respectively (a); sketch map of the 528-m CITIC Tower (b); mass concentration and aerosol composition of NR-$PM_{2.5}$ observed at the CITIC Tower (c); and comparisons of NO_2, SO_2, O_3, and $PM_{2.5}$ between the CITIC and NZG stations (d) during observational period (2020-2024).

The real-time chemical composition of non-refractory fine particles (NR-$PM_{2.5}$), including SO_4^{2-}, NO_3^-, NH_4^+, Chl^-, and Org, was measured with a ToF-ACSM (Aerodyne Co. Ltd., USA), which relies upon thermal vaporization and 70 eV electron-impact ionization (EI) (Jayne et al., 2000). The ambient particles were sampled into the ToF-ACSM through a University Research Glassware (URG) cyclone to remove coarse particles with a 2.5 μm size cutoff, followed by a Nafion dryer to dry the aerosols. Detailed operation principles of ToF-ACSM have been described in previous work (Frohlich et al., 2013; Williams et al., 2013).

https://doi.org/10.5194/egusphere-2026-801
Preprint. Discussion started: 13 March 2026

The mass concentration of $PM_{2.5}$ was monitored by an R&P model 1400a Tapered Element Oscillating Microbalance (TEOM, Thermo Scientific Co., USA). The collocated gaseous species, including SO_2, NO_x, and O_3, were measured by various gas analyzers (Thermo Scientific Co., USA). Additionally, ground level observations at NZG station of Beijing Environmental Protection Bureau were analyzed, including $PM_{2.5}$, SO_2, NO_2, and O_3. The NZG station is located at north of the CITIC with a distance of 4 km (Fig.1). The HYSPLIT model (Draxler and Hess, 1998) is used to determine sources of pollutants and transport routes of air masses arriving at the receptor site, and Global Data Analysis System (GDAS) outputs with 1 °×1 °resolution are used as input (Stein et al., 2015).

3. Results and Discussion

3.1 Aerosol composition in the 528-m layer over Beijing

The observations at the CITIC station were conducted mainly in autumn, winter and spring, with a total of 546 days from October 2020 to December 2024 (Table 1). The mean mass concentration of NR-$PM_{2.5}$ at the CITIC station was 19.14 μg m^{-3} during observational period (Fig.1c). The mass concentrations of Org, SO_4^{2-}, NO_3^-, NH_4^+, and Chl^- were 7.04, 2.00, 6.67, 3.04, and 0.40 μg m^{-3} respectively, accounting for 36.77%, 10.45%, 34.84%, 15.87%, and 2.01% in mass fraction. The fraction of SIAs, including SO_4^{2-}, NO_3^-, and NH_4^+, was 61.15% in NR-$PM_{2.5}$. This proportion is notably higher than observations at ground stations in urban Beijing. For example, in the observation of Ma et al. (2021), SIAs mass fraction ranged from 42% to 56% during two months experiment in Beijing (from January 14 to March 6, 2019). Seasonal aerosol composition in Beijing during 2012 to 2018 shows SIAs mass fractions were 52%, 55%, 49%, and 45% in spring, summer, autumn, and winter, respectively (Zhou et al., 2020).

Table 1. Total Observation days at the CITIC station during 2020 to 2024

	Month												
Year	1	2	3	4	5	6	7	8	9	10	11	12	Total (d)
2020	—	—	—	—	—	—	—	—	—	15	20	2	37
2021	12	23	1	—	—	—	—	—	—	10	30	31	107
2022	31	28	31	30	15	—	—	—	8	19	—	—	162
2023	—	—	9	30	29	15	21	—	—	—	—	—	104
2024	31	16	3	30	22	—	—	—	—	5	23	6	136

Aerosols typically decrease during the daytime due to enhanced vertical dispersion associated with PBL growth (Quan et al., 2013; Zhou et al., 2020). In contrast, diurnal variations in aerosol components at the CITIC station were remarkably weak (Fig.2). The fraction of SIAs exhibited a slight decrease around noon, likely driven by an increase in Org, which rose from 6.8 μg m^{-3} at 08:00 to 7.8 μg m^{-3} at 12:00 (Fig.2c).

https://doi.org/10.5194/egusphere-2026-801
Preprint. Discussion started: 13 March 2026

This morning increase in Org contrasts with the decreasing trend observed at ground level (Zhou et al., 2020).

For SO_4^{2-}, its concentration increased slightly in daytime, which was also contrary to typically decreasing trend at ground (Zhou et al., 2020), suggesting enhanced sulfate production in the 528-m layer during daytime. Liu et al. (2025) reported high H_2O_2 concentration in the 528-m layer, which can significantly enhance sulfate production, with estimated daytime formation rates of 0.2-1.1 μg m^{-3} h^{-1}. NO_3^- remained high level at night but decreased slightly in daytime, likely due to efficient nocturnal NO_3^- formation via dinitrogen pentoxide (N_2O_5) hydrolysis. Ma et al. (2023) indicate nocturnal NO_3^- formation via N_2O_5 hydrolysis in the high layer over Beijing was more efficient than at ground level, and could even exceed daytime photochemical nitrate formation. The diurnal variation of NH_4^+ was similar to that of NO_3^-.

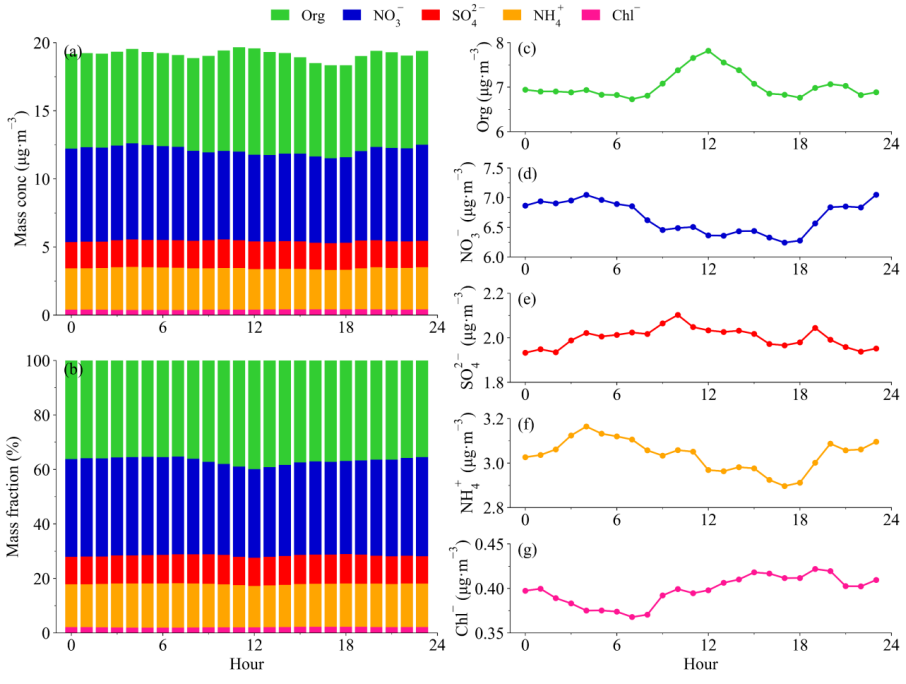

Figure 2. Diurnal variations of mass concentrations (a) and fraction (b) of NR-$PM_{2.5}$ and each component (c-g) during observational period (2020-2024).

These observations indicate that aerosol composition in the 528-m layer over Beijing differs clearly from that reported at ground level. Compared to ground level, pollutants at this altitude are more strongly influenced by regional transport. To examine this, we compared measurements between the CITIC station and the nearby ground-level NZG station, located approximately 4 km to the north (Fig.1a). Due to the lack of concurrent aerosol composition measurements at ground station in the

https://doi.org/10.5194/egusphere-2026-801
Preprint. Discussion started: 13 March 2026

same period, only $PM_{2.5}$ and gaseous pollutants were compared. As shown in Fig.1d, $PM_{2.5}$ at the CITIC station (34.8 μg m^{-3}) was lower than that at the NZG station (42.2 μg m^{-3}) while O_3 showed the opposite trend. For NO_2 and SO_2, NO_2 at the CITIC station (15.9 ppb) was 10.4% lower than that at the NZG station (17.7 ppb), while SO_2 showed a contrasting pattern. SO_2 in the 528-m layer (2.6 ppb) was 130% higher than that at the NZG station (1.1 ppb). As a megacity with 7 million vehicles, NO_x, including NO_2 and NO, are key atmospheric pollutants to air quality in Beijing. Vehicle-emitted NO_2 is rapidly diluted through vertical mixing, explaining its lower concentrations aloft. In contrast, SO_2 emissions in Beijing have been stringently controlled over the past decade. Consequently, ambient SO_2 is now predominantly derived from regional transport rather than local sources (Zhang et al., 2019). The observed pattern—enhanced SO_2 and reduced NO_2 in the 528-m layer relative to ground—confirms that pollutants in the 528-m layer over Beijing are influenced by a combination of regional transport and vertical mixing of locally emitted pollutants.

During regional transport, gaseous pollutants such as SO_2, NO_2, and NH_3 undergo chemical reactions to form SIAs, resulting in a high SIAs fraction in the 528-m layer. Aerosols and their precursors vary substantially across regions due to differences in source and atmospheric processing. Consequently, aerosol components over Beijing are expected to differ depending on the origin of incoming air masses. To improve our understanding of these processes, aerosol composition under distinct transport pathways is analyzed in the following sections.

3.2 Aerosol composition under different transport pathways

To investigate the regional transport of fine particles to Beijing, the HYSPLIT model (Draxler and Hess, 1998) was used to identify the source regions and transport pathways of air masses arriving at Beijing. Fig.3 shows the six clustered transport routes. Clusters 1, 3, and 5 correspond to air masses originating from the northwest of Beijing, whereas Clusters 2, 4, and 6 correspond to air masses originating from the south, northeast, and west of Beijing. The trajectory lengths of each cluster reflect the transport speed of the air masses: longer trajectories indicate faster movement. This is corroborated by the mean wind speeds in Beijing under each cluster (Table 2). Wind speeds were higher for Clusters 1 (3.62 m s^{-1}), 3 (2.98 m s^{-1}), and 5 (4.08 m s^{-1}) compared to Clusters 2 (2.23 m s^{-1}), 4 (2.70 m s^{-1}), and 6 (2.40 m s^{-1}). The spatial distribution of potential source contributions in the six clusters was consistent with this classification (Fig.4).

https://doi.org/10.5194/egusphere-2026-801
Preprint. Discussion started: 13 March 2026

Table 2. The mean wind speed at NZG station, and temperature and RH at the CITIC station in the six clusters

Cluster	Ground WS(m/s)	528m Temp(°C)	528m RH(%)
C1	3.62	8.33	26.36
C2	2.23	12.94	54.05
C3	2.98	6.43	35.41
C4	2.70	9.31	55.42
C5	4.08	2.8	26.21
C6	2.40	4.82	34.10

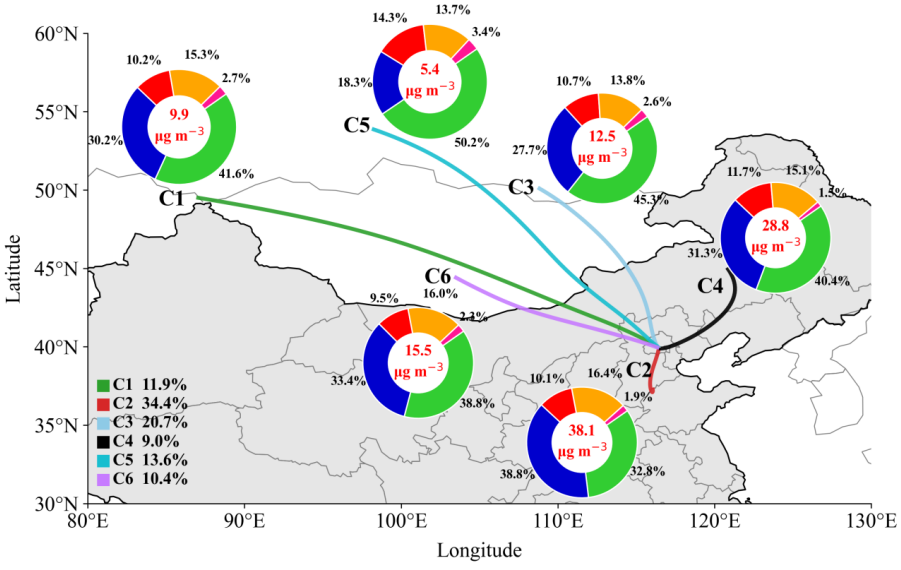

Figure 3. Forty-eight hours back trajectories of air masses over Beijing at altitude of 500 meters in the six clusters (C1-C6), together with NR-$PM_{2.5}$ mass concentration and composition in each cluster.

The mass concentrations of NR-$PM_{2.5}$ were 9.9 μg m^{-3}, 12.5 μg m^{-3}, and 5.4 μg m^{-3} in Clusters 1, 3, and 5, respectively—substantially lower than in Clusters 2 (38.1 μg m^{-3}), 4 (28.8 μg m^{-3}), and 6 (15.5 μg m^{-3}). These results are consistent with regional emission patterns. The northwestern source regions (including northwestern China, Mongolia, and Siberia) are relatively pristine, and air masses from these areas delivered cleaner air to Beijing. Strong winds associated with these clusters also enhanced the dispersion of local pollutants, further contributing to lower aerosol loading. In contrast, air masses arriving from the south, northeast, and west originated from heavily polluted regions, thereby transporting polluted air to Beijing. Weaker winds under these clusters favored the accumulation of locally emitted pollutants. Besides mass concentrations, distinct differences in aerosol chemical composition were observed in the six clusters. The fraction of SIAs was lower in the three northwestern clusters—55.7% (Cluster 1), 52.1% (Cluster 3), and 46.3%

https://doi.org/10.5194/egusphere-2026-801
Preprint. Discussion started: 13 March 2026

(Cluster 5) —compared to the other three clusters: 65.2% (Cluster 2), 58.1% (Cluster 4), and 59.0% (Cluster 6) (Fig.3). Organic aerosol fractions exhibited the opposite trend. Among SIAs, the northwestern clusters showed lower NO_3^- and NH_4^+, but higher SO_4^{2-} contributions. Specifically, NO_3^- accounted for 30.2%, 27.7%, and 18.3% of NR-$PM_{2.5}$ in Clusters 1, 3, and 5, respectively—lower than in Clusters 2 (38.8%), 4 (31.3%), and 6 (33.4%). Conversely, SO_4^{2-} fractions were higher in the northwestern clusters (10.2%, 10.7%, and 14.3%) than in Clusters 2 (10.1%) and 6 (9.5%), though slightly lower than in Cluster 4 (11.7%). NH_4^+ reached its highest fraction in Cluster 2 (16.4%).

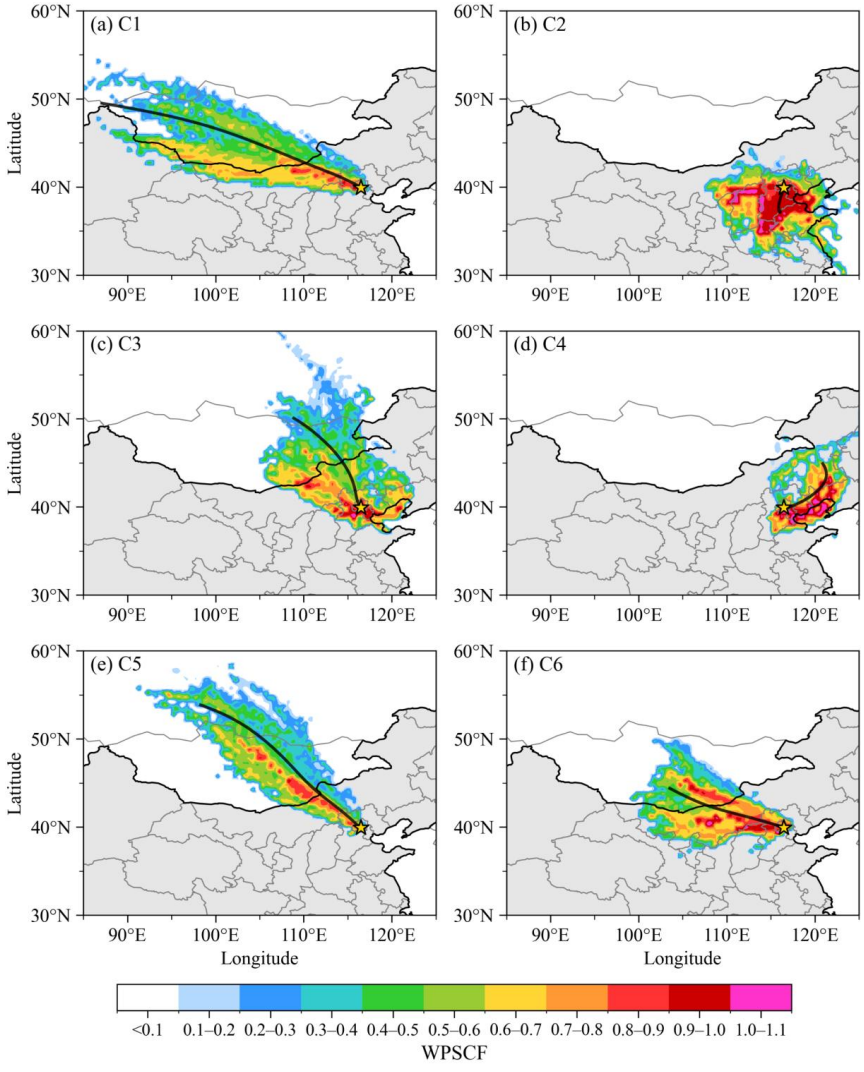

Figure 4. Potential source contribution at altitude of 500 m over Beijing in the six clusters

https://doi.org/10.5194/egusphere-2026-801
Preprint. Discussion started: 13 March 2026

In addition to aerosol composition, differences of $PM_{2.5}$, and gas pollutants in the six clusters were also examined (Fig.5). Similar to NR-$PM_{2.5}$, $PM_{2.5}$ concentrations exhibited pronounced variability among the six clusters, ranging from a maximum of 71.5 μg m^{-3} in Cluster 2 to a minimum of 12.7μg m^{-3} in Cluster 5, yielding a maximum-to-minimum of 5.62. In contrast, SO_2 showed much weaker variability, with concentrations ranging from 2.96 ppb (Cluster 2) to 2.02 ppb (Cluster 5), corresponding to a ratio of only 1.47. NO_2 variability was moderate, with a maximum of 22.09 ppb in Cluster 2 and a minimum of 9.73 ppb in Cluster 5 (ratio = 2.27). To access the relative contributions of SO_2 and $PM_{2.5}$ under different transport clusters, the $SO_2/PM_{2.5}$ ratio was calculated. The ratio was higher in the three clusters originating from the northwest—0.10 ppb μg^{-1} m^3 (Cluster 1), 0.11 ppb μg^{-1} m^3 (Cluster 3), and 0.16 ppb μg^{-1} m^3 (Cluster 5)—than in the other three clusters: 0.04 ppb μg^{-1} m^3 (Cluster 2), 0.07 ppb μg^{-1} m^3 (Cluster 4), and 0.07 ppb μg^{-1} m^3 (Cluster 6). This indicates that northwesterly air masses carried relatively less $PM_{2.5}$, but proportionally more SO_2, consistent with the enhanced sulfate mass fractions observed in aerosols under these clusters (Fig.3).

https://doi.org/10.5194/egusphere-2026-801
Preprint. Discussion started: 13 March 2026

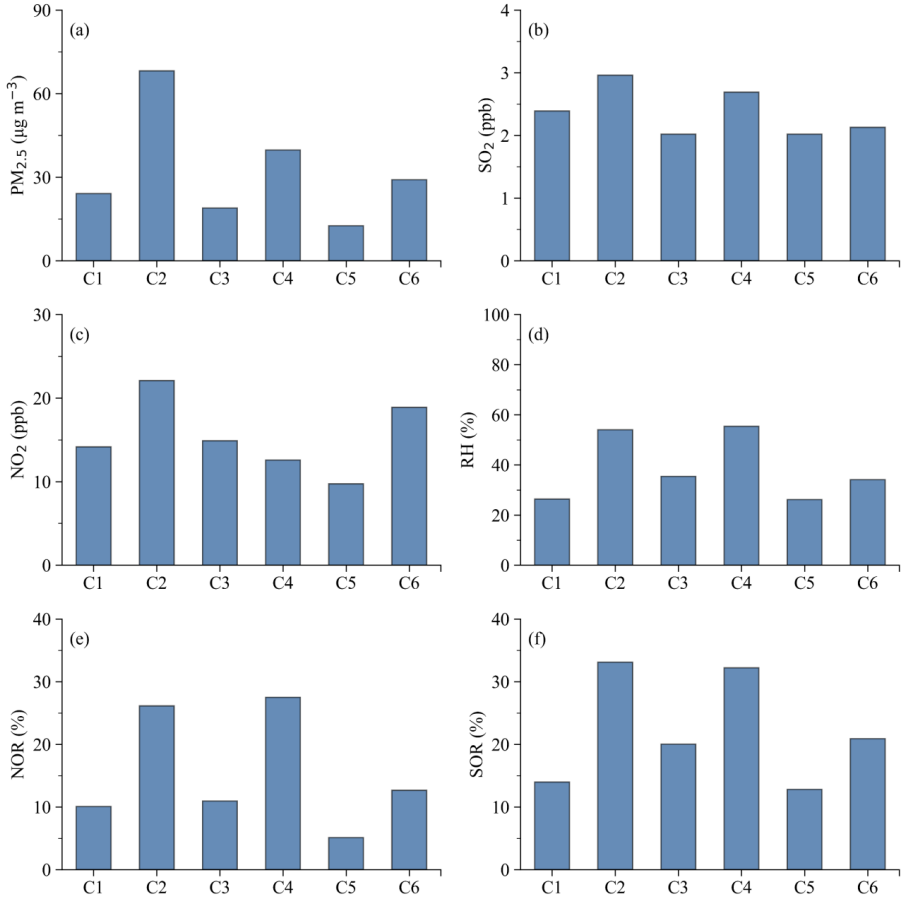

Figure 5. Variations of $PM_{2.5}$, SO_2, NO_2, RH, NOR and SOR in the six clusters, respectively.

The distinct pollutants across clusters reflect the differing emission characteristics of their source regions. Air masses originating from the northwest exhibited a high sulfate mass fraction in aerosols and relatively high SO_2, suggesting that coal combustion dominates emissions in this region. In contrast, air masses from the south and northeast carried higher $PM_{2.5}$, thereby exacerbating air pollution in Beijing. Regarding aerosol composition, the mass fraction of SIAs increased when air masses arrived from the south and northeast. NO_3^- is form through the oxidation of NO_x, which is predominantly emitted from combustion-related sources—primarily vehicle exhaust, coal combustion, and biomass burning. Similarly, NH_4^+ derives from the neutralization of NH_3, which is mainly released from combustion-related sources, agricultural activities (e.g., fertilized soils and animal waste), natural soils, and nitrogen-enriched water bodies (Chen et al., 2022). Consequently, emissions in the southern and northeastern regions are more complex, involving contributions from coal combustion, vehicle exhaust, agricultural practices, and natural sources.

https://doi.org/10.5194/egusphere-2026-801
Preprint. Discussion started: 13 March 2026

Gaseous pollutants can be converted to particles during transport through photochemical and heterogeneous reactions. To access the influence of chemical reactions on aerosol composition in the six clusters, oxidation ratios of nitrogen (NOR) and sulfur (SOR) were calculated. The NOR and SOR were defined as the ratios of particle phase of nitrogen and sulfur to total nitrogen and sulfur (both gas and particle phases), respectively (Chen et al., 2015). As shown in Fig.5f, SOR values were higher in Clusters 2 (0.33) and 4 (0.32) than in Clusters 1 (0.14) and 5 (0.13). A similar pattern was observed for NOR (Fig.5e). These differences may be primarily attributed to variations in RH among the six clusters (Fig.6). RH increased markedly when air masses originated from the south and northeast (Fig.5d), which likely promoted aqueous-phase heterogeneous oxidation of both SO_2 and NO_2 (Pathak et al., 2011; Ma et al., 2021, 2023). Collectively, these results indicate that the observed differences in aerosol composition over Beijing in the six transport clusters are governed by a combination of regional emission sources and chemical reactions during transport.

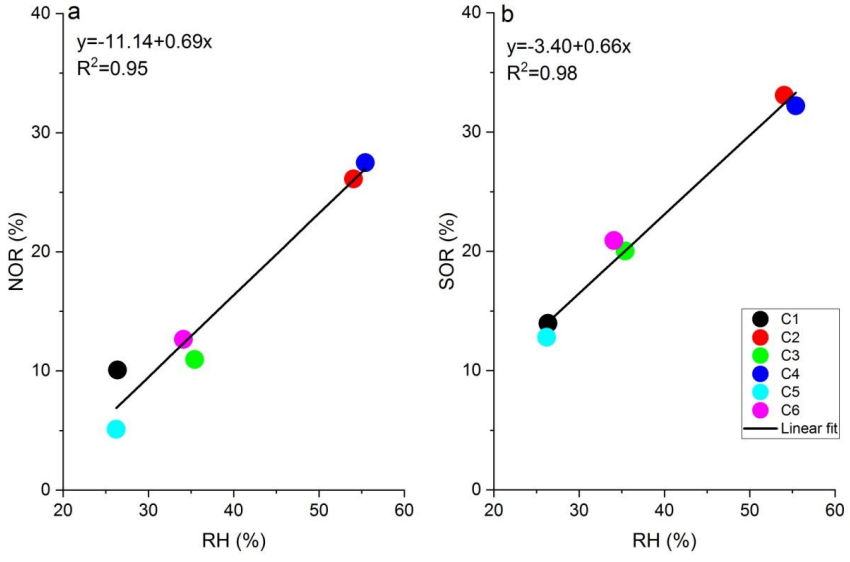

Figure 6. Relationships of the NOR (a), SOR(b) to RH. The colors of dot represent distinct clusters as shown in Fig.3.

3.3 Seasonal aerosol composition

As shown in Fig.7, both mass concentration and fraction of NR-$PM_{2.5}$ reflected clear seasonal variations. The mass concentration was lowest in summer (9.8 μg m^{-3}), followed by winter (15.6 μg m^{-3}), spring (20.6 μg m^{-3}) and autumn (25.4 μg m^{-3}). In summer, frequent precipitation enhanced wet deposition, while increased atmospheric instability promoted vertical diffusion of pollutants, resulting in low aerosol concentration. NO_3^- mass fraction was lowest in summer (15.1%), likely due to its

https://doi.org/10.5194/egusphere-2026-801
Preprint. Discussion started: 13 March 2026

semi-volatile property; gas-particle partitioning of nitrate is strongly temperature-dependent, and higher temperature favors the gaseous phase, thereby reducing particulate nitrate. In contrast, SO_4^{2-} mass fraction peaked in summer (21.9%), likely due to enhanced aqueous reactions under high RH (Zhang et al., 2018b). In autumn, atmospheric instability decreases gradually with decreasing solar radiation, leading to aerosol accumulation. For aerosol components, NO_3^- mass fraction increased to 37.9%, while SO_4^{2-} decreased to 8.1%, likely driven by concurrent decreases in temperature and RH. In winter and spring, SO_4^{2-} mass fraction increased again (to 10.9% on average), primarily due to increased SO_2 emissions from intensified coal combustion for residential heating. These observations demonstrate that marked seasonal variations in aerosol species over Beijing are closely linked to differences in emission sources and formation mechanisms.

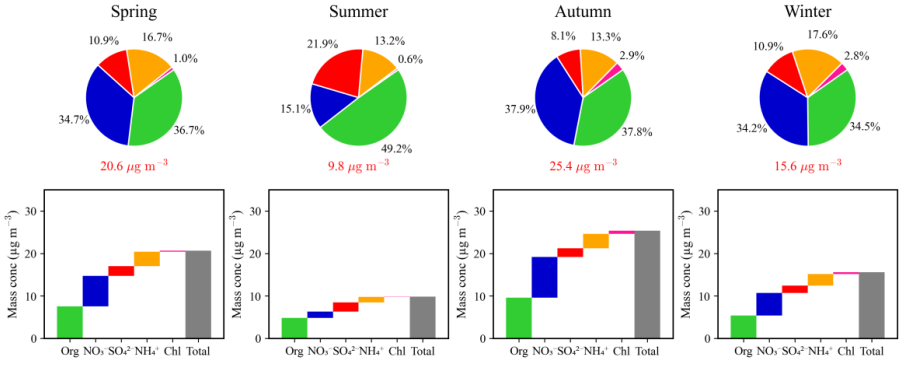

Figure 7. The mean mass concentration and composition of NR-$PM_{2.5}$ in four seasons during observational period (2020-2024).

As discussed in section 3.2, aerosols in the 528-m layer are strongly influenced by regional transport. To further examine how transport pathways modulate aerosol properties across seasons, we analyzed differences in both mass concentration and chemical composition under distinct air mass trajectories (Fig.8). Due to limited samples, air mass origins were classified into four clusters for each season. In summer, SO_4^{2-} mass fraction exceeded that of NO_3^- in three of the four clusters, with the exception of Cluster 1. Specially, SO_4^{2-} accounted for 23.0%, 15.3%, 15.7%, and 23.6% , while NO_3^- accounted for 23.8%, 5.8%, 8.5%, and 11.9% in Clusters 1-4, respectively. Notably, the two clusters originating from the south (Clusters 1 and 4) exhibited higher SO_4^{2-} fractions than the northwest-derived cluster (Cluster 3). This reversal of the typical pattern is likely attributable to enhanced sulfate formation through aqueous-phase oxidation, as southerly airflows in summer transport moist air masses into Beijing (Fig.5d).

In autumn, NO_3^- mass fraction increased while SO_4^{2-} decreased sharply in all four clusters. Specifically, SO_4^{2-} accounted for 8.1%, 13.0%, 6.9%, and 8.1%, whereas NO_3^- accounted for 29.3%, 16.5%, 40.3%, and 40.7% in Clusters 1-4, respectively.

https://doi.org/10.5194/egusphere-2026-801
Preprint. Discussion started: 13 March 2026

Consistent with the pattern shown in Fig.3, NR-$PN_{2.5}$ mass concentrations were higher in the south-originating cluster (Cluster 3, 40.7 μg m^{-3}) and west-originating cluster (Cluster 4, 31.8 μg m^{-3}) than in the two northwest-originating clusters (Cluster 1, 9.7 μg m^{-3}; Cluster 2, 10.2 μg m^{-3}). In terms of aerosol composition, the two northwest-originating clusters exhibited lower NO_3^-, but higher SO_4^{2-} fractions. In winter and spring, SO_4^{2-} mass fraction increased slightly in all four clusters. Consistent with autumn, NR-$PN_{2.5}$ concentrations in the northwest-originating cluster were lower than those in clusters arriving from the south and northeast. Similarly, aerosols in the northwest-originating clusters consistently showed lower NO_3^- and higher SO_4^{2-} fractions. These results demonstrate that seasonal variations in aerosol composition over Beijing are governed by differences in emission sources, formation mechanisms, and the influence of regional transport.

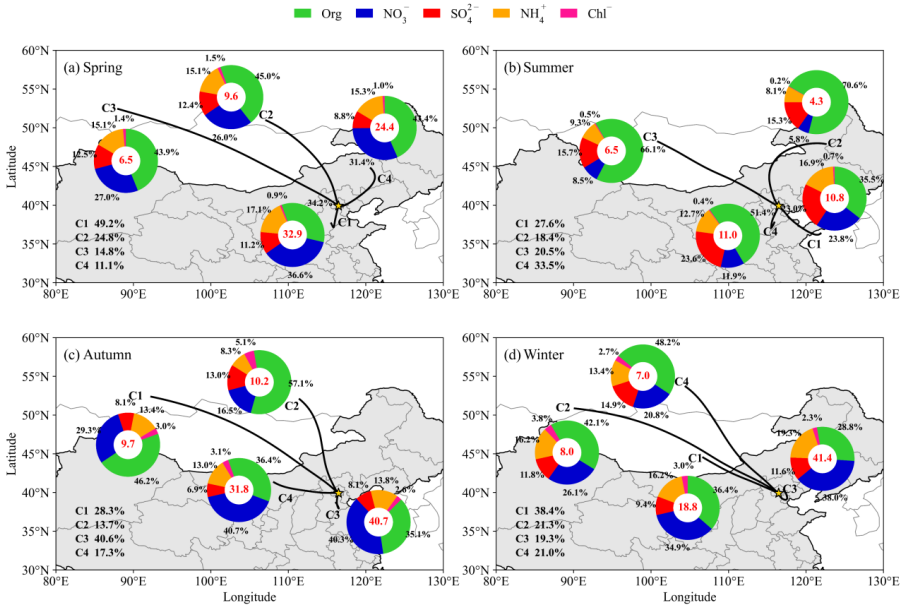

Figure 8. Forty-eight hours back trajectories of air masses over Beijing at altitude of 500 meters in four seasons, together with mass concentration and composition of NR-$PM_{2.5}$ in each cluster.

3.4 Vertical mixing of pollutants through the PBL process

Regional pollutants may be transported downwards, thereby exacerbating air pollution in Beijing. To understand this process, diurnal variations of pollutants at the two stations were investigated. Due to the lack of concurrent aerosol composition measurements at ground station in the same period, only $PM_{2.5}$ and gaseous pollutants were compared. Observations showed the differences of pollutants between the two stations decreased in the daytime but increased at night, particularly for gaseous pollutants (Fig.9). At the NZG station, NO_2 remained high concentration at night and

https://doi.org/10.5194/egusphere-2026-801
Preprint. Discussion started: 13 March 2026

decreased in the morning, and reached a minimum of 11.0 ppb around 15:00. After that, its concentration gradually increased. In contrast, NO_2 at the CITIC station exhibited an opposite diurnal pattern. NO_2 increased in the morning, peaked at 13:00 (17.3 ppb), and then decreased, remaining low concentration throughout the night. SO_2 showed a contrasting trend to NO_2. At the NZG station, SO_2 increased in the morning, peaked at 13:00 (1.36 ppb), then decreased and kept in low concentration at night. However, SO_2 was relatively stable, with only a slight decrease around noon, at the CITIC station. O_3 also exhibited marked differences between the two stations; its concentration at the NZG station was close to the CITIC in daytime, but much lower than the latter at night (Fig.9c), likely due to NO titration (Brown and Stutz, 2012). Compared with short-lived gaseous pollutants, the difference in $PM_{2.5}$ between the two stations was less significant (Fig.9d).

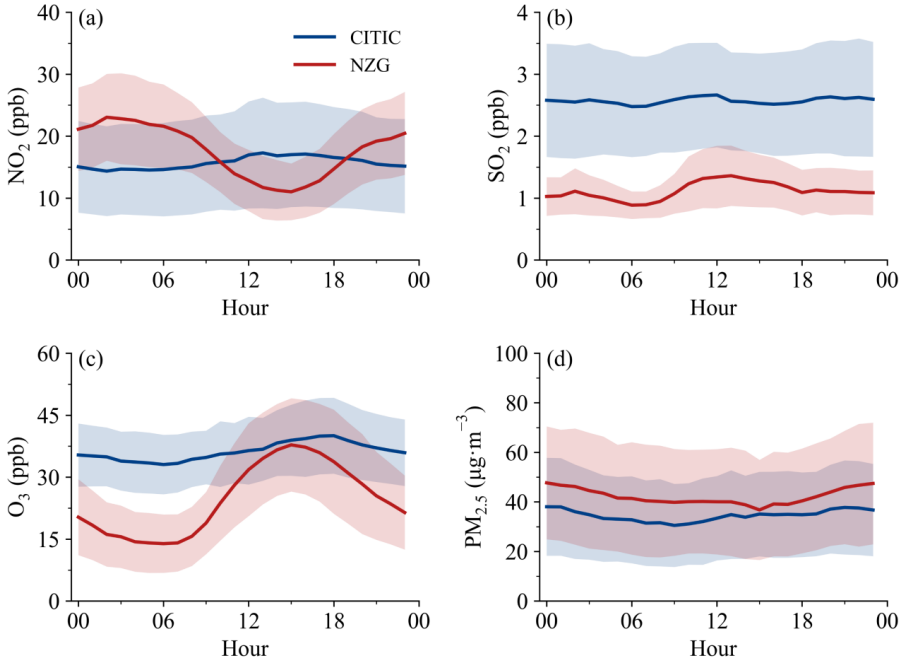

Figure 9. Diurnal variations of NO_2, SO_2, O_3, and $PM_{2.5}$ during observational period (2020-2024) at the CITIC (blue) and NZG (red) stations, respectively. The shaded areas denote standard deviation.

The opposite patterns of NO_2 and SO_2 at the two stations may be caused predominantly by the PBL process. Our previous studies show that the CITIC station resides in the residual layer (RL) at night (Ma et al., 2023; Quan et al., 2025). The decoupling between the RL and nocturnal stable boundary layer (SBL) substantially suppresses vertical exchange of pollutants between the two layers, leading to large differences of pollutants between the CITIC and NZG stations. In the morning, the daytime convective boundary layer (CBL) develops gradually under increasing solar radiation, and eventually couples the overlying RL. This coupling strongly enhances

https://doi.org/10.5194/egusphere-2026-801
Preprint. Discussion started: 13 March 2026

vertical mixing of pollutants. In this process, locally emitted NO_2 at ground level was upwards transported, leading to the contrasting diurnal patterns of NO_2 between the two stations. By contrast, regional transported SO_2 was transported downwards in this process. Notably, NO_2 at the CITIC exceeded that at the NZG between 11:00 and 18:00, likely due to the conversion of NO to NO_2 during vertical mixing in the presence of high O_3 concentration aloft (Fig.9c). For $PM_{2.5}$, its difference between the two stations also decreased at afternoon (Fig.9d), consistent with enhanced vertical mixing in this period. These results indicate that regional transported pollutants in high layer were downwards transported to ground dominantly via PBL process, thereby exacerbating air pollution in Beijing.

4 Summary

Regional transport of pollutants to Beijing was investigated in this study based on comprehensive observations of aerosol components and gaseous pollutants conducted at a unique 528-m platform over urban Beijing from 2020 to 2024. The main findings are summarized as follows:

(1) Aerosol mass concentration and chemical composition varied markedly with air mass origin. Air masses from the northwest delivered relatively clean air to Beijing, characterized by low aerosol levels but relatively high SO_2. In terms of composition, these northwesterly flows exhibited lower NO_3^- and NH_4^+ fractions but higher SO_4^{2-} and Chl^-. In contrast, air masses from the south, and northeast transported high aerosols with increased SIAs fractions, including NO_3^-, NH_4^+, and SO_4^{2-}. These results suggest that emissions in the northwest are dominated by coal combustion, whereas those in the south and northeast involve multiple sources, including coal combustion, vehicle exhaust, agricultural and natural soils, and animal waste.

(2) Both the SOR and NOR were higher in air masses originating from the south and northeast than in those from the northwest, likely due to higher RH in the former, which promotes aqueous-phase heterogeneous oxidation of SO_2 and NO_2. These results indicate that differences in aerosol properties in the six transport pathways are governed by a combination of regional emissions and chemical reactions during transport.

(3) Contrasting diurnal patterns of SO_2 and NO_2 between the 528-m layer and ground level confirm that pollutants are well mixed during the day but strongly suppressed at night due to the decoupling of the RL and SBL. Driven by the development of PBL, locally emitted NO_2 is transported upward during daytime, while regionally derived SO_2 aloft is transported downward toward the surface. These findings demonstrate that regional aerosols over Beijing are transported downward primarily through PBL processes, thereby exacerbating surface air pollution.

Acknowledgments

This research is supported by National Natural Science Foundation of China (42475122), Beijing Natural Science Foundation (8242027), Key Projects in the National Science and Technology (2023YFC3711000) and Beijing Nova Program (20250484803).

https://doi.org/10.5194/egusphere-2026-801
Preprint. Discussion started: 13 March 2026

Author Contribution JQ and PT initiated and conceived the research; JQ, XL and PM led the observations, analyses and writing; YP and QW analyzed the data; PT and LZ revised the manuscript.

Data availability. The observational data at the CITIC station are available from https://doi.org/10.5281/zenodo.18424062 (Quan, 2026). Pollutant data ($PM_{2.5}$, SO_2, NO_2 and O_3) at NZG station are available from the China National Environmental Monitoring Centre (http://www.cnemc.cn/).

Competing interests

The authors declare that they have no competing interests.

Reference

Brown, S. S., and Stutz, J.: Nighttime radical observations and chemistry, Chemical Society Reviews, 41(19), 6405-6447, https://doi.org/10.1039/c2cs35181a, 2012.

Chen, C., Sun, Y.L., Xu, W.Q., Du, W., Zhou, L.B., Han, T.T., Wang, Q.Q., Fu, P.Q., Wang, Z.F., and Gao, Z.Q.: Characteristics and sources of submicron aerosols above the urban canopy (260 m) in Beijing, China during 2014 APEC summit, Atmos. Chem. Phys., 15 (16), 22889-22934, 2015.

Chen, Z., Song, W., Hu, C., Liu, X., Chen, G., Walters, W. W., Michalski, G., Liu, C., Fowler, D., and Liu, X.: Significant contributions of combustion related sources to ammonia emissions, Nature communication, 13, 7710, https://doi.org/10.1038/s41467-022-35381-4, 2022.

Draxler, R.R., and Hess, G.D.: An overview of the HYSPLIT_4 modeling system for trajectories, dispersion, and deposition, Aust. Met. Mag., 47, 295-308, 1998.

Du, H., Li, J., Chen, X., Wang, Z., Sun, Y., Fu, P., Li, J., Gao, J., and Wei, Y.: Modeling of aerosol property evolution during winter haze episodes over a megacity cluster in northern China: roles of regional transport and heterogeneous reactions of SO_2, Atmos. Chem. Phys., 19, 9351-9370, 2019.

Frohlich, R., Cubison, M. J., Slowik, J. G., Bukowiecki, N., Prevot, A. S. H., Baltensperger, U., Schneider, J., Kimmel, J. R., Gonin, M., Rohner, U., Worsnop, D. R., and Jayne, J. T.: The ToF-ACSM: a portable aerosol chemical speciation monitor with TOFMS detection, Atmospheric Measurement Techniques, 6(11), 3225-3241, 2013.

Kang, Z., Ma, P., Quan, J.N., Jia, X., Liao, Z., Cheng, Z., Wang, Q., Dai, L., Zhao, X., Zhang, Z., Yuan, T., and Pan, Y.: Observational evidence of the regional transported black carbon in high layer over Beijing, Atmospheric Environment, 311, 120000, 2023.

Jayne, J.T., Leard, D.C., Zhang, X., Davidovits, P., Smith, K.A., Kolb, C.E., and

https://doi.org/10.5194/egusphere-2026-801
Preprint. Discussion started: 13 March 2026

Worsnop, D.R.: Development of an Aerosol Mass Spectrometer for Size and Composition Analysis of Submicron Particles, Aerosol Sci. Technol., 33, 49-70, 2000.

Li, J., Wang, Z., Huang, H., Hu, M., Meng, F., Sun, Y., Wang, X., Wang, Y., and Wang, Q.: Assessing the effects of trans-boundary aerosol transport between various city clusters on regional haze episodes in spring over East China, Tellus B., 65 (1), 20052, 2013.

Li, Y., Ye, C., Liu. J., Zhu, Y., Wang, J., Tan, Z., Lin, W., Zeng, L., and Zhu, T.: Observation of regional air pollutant transport between the 2 megacity Beijing and the North China Plain, Atmos. Chem. Phys., 16, 14265-14283, http://doi:10.5194/acp-2016-476, 2016.

Li, P., Yan, R., Yu, S., Wang, S., Liu, W., and Bao, H.: Reinstate regional transport of $PM_{2.5}$ as a major cause of severe haze in Beijing, PNAS, 112, 2739-2740,www.pnas.org/cgi/doi/10.1073/pnas.1502596112, 2015.

Liu Q., Quan, J.N., Jia, X.C., Sun, Z., Li, X., Gao, Y., and Liu, Y.: Vertical profiles of aerosol composition over Beijing, China: Analysis of in-situ aircraft measurements, J. Atmos. Sci., 76, 231-245, 2019.

Liu, P., Jia, S., Li, S., Ma, P., Ma, Y., Liu, Y., Liao, Z., Wang, Y., Chu, B., Ma, Q., Quan, J., Mu, Y., and He, H.: Unexpectedly high levels of H_2O_2 drive sulfate formation over the residual layer in Beijing, Environmental Science and Technology, 59(9) DOI: 10.1021/acs.est.4c09004, 2025.

Ma, P., Quan, J.N., Jia, X., Liao, Z., Wang, Q., Cheng, Z., Dou, Y., Su, J., Pan, Y.: Effects of ozone and relative humidity in secondary inorganic aerosol formation during haze events in Beijing, China, Atmospheric Research, 264, 105855, 2021.

Ma, P., Quan, J.N., Dou, Y., Pan, Y., Liao, Z., Cheng, Z., Jia, X., Wang, Q., Zhan, J., Ma, W., Zheng, F., Wang, Y., Zhang, Y., Hua, C., Yan, C., Kulmala, M., Liu, Y., Huang, X., Liu, Y., Brown, S. S., Liu, Y., Brown, S. S., and Liu, Y.: Regime-dependence of nocturnal nitrate formation via N_2O_5 hydrolysis and its implication for mitigating nitrate pollution, Geophysical Research Letters, 50, e2023GL106183. https://doi.org/10.1029/2023GL106183, 2023.

Pathak, R.K., Wang, T., and Wu, W.S.: Nighttime enhancement of $PM_{2.5}$ nitrate in ammonia-poor atmospheric conditions in Beijing and Shanghai: Plausible contributions of heterogeneous hydrolysis of N_2O_5 and HNO_3 partitioning, Atmos. Environ., 45 (5), 1183-1191, 2011.

Quan, J.N., Gao, Y., Zhang, Q., Tie, X., Cao, J., Han, S., Meng, J., Chen, P., and Zhao, D.: Evolution of planetary boundary layer under different weather conditions, and its impact on aerosol concentrations, Particuology, 11, 34-40, 2013.

Quan, J.N., Dou, Y., Zhao, X., Liu, Q., Sun, Z., Pan, Y., Jia, X., Cheng, Z., Ma, P., Su, J., Xin, J., and Liu, Y.: Regional atmospheric pollutant transport mechanisms

https://doi.org/10.5194/egusphere-2026-801
Preprint. Discussion started: 13 March 2026

over the North China Plain driven by topography and planetary boundary layer processes, Atmos. Environ., 221, 117098, https://doi.org/10.1016/j.atmosenv.2019.117098, 2020.

Quan, J.N., Ma, P., Pan, Y., Cheng, S., Wang, Q., Lan, L., Dai, L., Wang, Y., and Liu., Y.: Vertical mixing of pollutants and secondary inorganic aerosol formations over Beijing, China, Atmospheric Environment, 357, 121312, 2025.

Quan, J.N.: Observations at CITIC station, Beijing during 2020 to 2024, Zenodo [data set], https://doi.org/10.5281/zenodo.18424062, 2026.

Stein, A.F., Draxler, R.R., Rolph, G.D., Stunder, B.J.B., Cohen, M.D., and Ngan, F.: NOAA'S HYSPLIT atmospheric transport and dispersion modeling system, Bull. Am. Meteorol. Soc., 96 (12), 2059-2077, 2015.

Sun, P., Nie, W., Chi, X., Huang, X., Ren, C., Xue, L., Shan, Y., Wen, L., Li, H., Chen, T., Qi, Y., Gao, J., Zhang, Q., and Ding, A.: Aircraft study of secondary aerosols in long-range transported air masses from the North China Plain by a mid-latitude cyclone, Journal of Geophysical Research, 127, e2021JD036178. https://doi.org/10.1029/2021JD036178, 2022.

Tan, Q., Ge, B., Xu, X., Gan, L., Yang, W., Chen, X., Pan, X., Wang, W., Li, J., and Wang, Z.: Increasing impacts of the relative contributions of regional transport on air pollution in Beijing: Observational evidence, Environmental Pollution, 292, 118407, https://doi.org/10.1016/j.envpol.2021.118407, 2021.

Wang, S., Zhao, W., Xu, X., Fang, B., Zhang, Q., Qian, X., Zhang, W., Chen, W., Pu, W., and Wang, X.: Dependence of columnar aerosol size distribution, optical properties, and chemical components on regional transport in Beijing, Atmospheric Environment, 169, 128-139, 2017.

Williams, L. R., Gonzalez, L. A., Peck, J., Trimborn, D., McInnis, J., Farrar, M. R., Moore, K. D., Jayne, J. T., Robinson, W. A., Lewis, D. K., Onasch, T. B., Canagaratna, M. R., Trimborn, A., Timko, M. T., Magoon, G., Deng, R., Tang, D., Blanco, Edlr, Prevot, A. S. H., Smith, K. A., and Worsnop, D. R.: Characterization of an aerodynamic lens for transmitting particles greater than 1 micrometer in diameter into the Aerodyne aerosol mass spectrometer, Atmospheric Measurement Techniques, 6(11), 3271-3280, 2013.

Zhang, H., Cheng, S., Wang, X., Yao, S., and Zhu, F.: Continuous monitoring, compositions analysis and the implication of regional transport for submicron and fine aerosols in Beijing, China. Atmos. Environ. 195, 30-45, https://doi.org/10.1016/j.atmosenv.2018.09.043, 2018a.

Zhang, Y., Tong, S., Ge, M., Jing, B., Hou, S., Tan, F., Chen, Y., Guo, Y., and Wu, L.: The influence of relative humidity on the heterogeneous oxidation of sulfur dioxide by ozone on calcium carbonate particles, Sci. Total Environ., 633, 1253–1262, 2018b.

https://doi.org/10.5194/egusphere-2026-801
Preprint. Discussion started: 13 March 2026

Zhang, Q., Zheng, Y., Tong, D., Shao, M., and Hao, J.: Drivers of improved PM2.5 air quality in China from 2013 to 2017, Proc. Natl. Acad. Sci., 116, 24463-24469, 2019.

Zhang, Z., Wang, S., Wang, P., Zhu, S., Zhang, H., and Wang, S.: Regional transport dominates air pollution events in all seasons in Beijing in 2020, Atmospheric Environment, 323(15), 120395, 2024.

Zhou, W., Xu, W., Kim, H., Zhang, Q., Fu, P., Worsnop, D. R., and Sun, Y.: A review of aerosol chemistry in Asia: insights from aerosol mass spectrometer measurements, Environ. Sci.: Processes Impacts, 2020, 22, 1616.